Effect of Mechanical Recycling on Structural Modification and Mechanical Behavior of PET

Gabriela Gonçalves Marques, Marion Colella, Aline Couffin, Philippe Hajji, Raber Inoubli, Véronique Bounor-Legaré, René Fulchiron

Effect of mechanical recycling on structural modification and mechanical behavior of PET

Gabriela Gonçalves Marques[1,2], Marion Colella[4], Aline Couffin[3], Philippe Hajji[2], Raber Inoubli[2], Véronique Bounor-Legaré[1], and René Fulchiron[1*]

[1]Universite Claude Bernard Lyon 1, INSA Lyon, Université Jean Monnet, CNRS UMR 5223, Ingénierie des Matériaux Polymères F-69622 Villeurbanne Cedex, France
[2]Arkema – Centre de Recherche Rhônes Alpes – CS42063, F-69491 Pierre Benite, France
[3]Arkema – Groupement de recherches de Lacq (GRL) – BP 34, 64170 Lacq, France
[4]Universite Claude Bernard Lyon 1, INSA Lyon, Université Jean Monnet, CNRS UMR 5223, Ingénierie des Matériaux Polymères F-69622 Villeurbanne Cedex, France
* Corresponding author: rene.fulchiron@univ-lyon1.fr

Abstract

Climate changes and the engendered environmental stress pressure the search for greener solutions. One striking example of the environmental stress is the plastic pollution [1]. Besides reducing the plastic consumption, recycling is today one of the applicable approaches [2]. In this context, polyethylene terephthalate (PET) is on the spotlight. More than having unique properties, PET occupies today the podium of the recycled polymers worldwide [2, 3]. However, despite the effort on PET recycling and the extensive number of published papers on that matter, many challenges are still restraining its development. One of the reasons for that is a lack of understating of the structural modifications caused by processing. Moreover, the impact of these changes both on the processing step and the final product properties. This study focused on the effect of mechanical recycling process on the mechanical response of PET. By successive cycles of extrusion and injection molding, recycled PET (rPET) could be produced and characterized. The widely described chain scission was confirmed by size exclusion chromatography. The consequent loss of viscosity was observed during the processing and by rheological measurements, rendering the process more and more challenging. A modification of the crystallization kinetics was also brought to light by different techniques such as differential scanning calorimetry and polarized light optical microscopy. Despite the different effects on the matrix, mechanical characterization showed a stable response. Tensile properties showed a very ductile material with more than 400% elongation for all virgin and rPET. The notched sensitivity of this material could also be observed on Izod impact test, remaining rather low but also stable. The better understanding of the relationship between structural modification and final properties may allow to fine tune impact modifiers structures for increasing rPET toughness and applications.

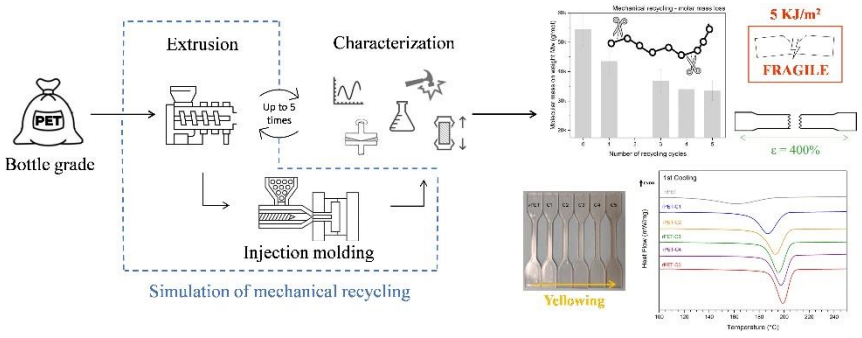

1 Introduction

The industrial development of plastics since the early 1950s has engendered a huge amount of waste. It is estimated that 6.3 billion tons of plastic waste were produced up to 2015 [1]. Of this total, 79% are now accumulated in landfills and natural environments, harming not only human health but wildlife as a whole [1, 2, 4]. Polyethylene terephthalate (PET), as one of the most used thermoplastics in the world, represents an important portion of this polymeric waste [2, 3, 5].

Recycling appears as one effective solution for dealing with this increasing waste management problem. But it represents today only 9% of the fate of polymeric waste [1]. The reasons for that are numerous: i) socio-economic challenges, such as deficient collection systems, ii) insufficient investments iii) non-competitive prices of reprocessed resins tend to restrain its development [6]. More than that, technical limitations come also as another key point slowing its development in an industrial scale.

Today the most well-established business for waste valorization of PET is mechanical recycling [6–8]. By using standard extrusion lines, it consists of the production of re-granulated materials for another life-cycle. The calculated carbon-footprint of this technique is considered to be lower than other methods such as advanced recycling or energy recovery [7]. However, even though mechanical recycling is already used in an industrial scale, technical challenges tend to limit the possible applications and increase the recyclate prices [6]. Keeping an economical interest and an ecological balance is essential for the thrive of this method [9].

During reprocessing, polyesters such as PET can suffer from several degradation mechanisms, such as hydrolysis or thermal-oxidative reaction for instance, that can modify their chemical structure [10, 11]. Several authors have studied the effect of multiple processing cycles on the chemical structure and rheological behavior of PET [12–20]. Some examples can be given for illustration. The results presented by Assadi et al. [12] demonstrated the processing difficulty after three single-screw extruder cycles (set at 40 rpm, with temperatures ranging from 240 to 280°C and a residence time of $\approx$ 1.3 minutes). With size exclusion chromatography (SEC) and rheological measurements, they showed that both chain scission and crosslinking can happen during recycling, initially leading to a decrease in molar mass in weight (Mw) and, after three cycles, evolving to a gel formation. This phenomenon was confirmed by Mark-Houwink plot with SEC data, where a shift between recycled and virgin PET plots can reasonably by explained by branching. After the forth cycle, the viscosity increase was associated to the number of branching reaching the gel point (order of magnitude of 18 mmol/kg). Even if expected to be very limited, the gel apparition can accumulate and lead to a crosslinking network that can be extremely problematic for a post-processing point of view. The use of antioxidants and additives for processing stability can be helpful but also lead to other drawbacks (secondary reactions, alterations in color and haze, instability during storing, etc.) [21–23]. Nevertheless, in this

work, no information was given about the mechanical response of the recycled material.

Spinacé and Paoli [17] confirmed the occurrence of degradation mechanisms for reprocessed PET (rPET) with the increase on the concentration of carboxyl end-groups (measured by titration) and the yellowing index. The engendered chain scission improved the chain mobility, shifting the crystallization temperature to higher values with measurements by differential scanning calorimetry (DSC) when cooling from the molten state. A crystallinity increase (between 24% to 38%) affected the mechanical response on a tensile test. A complete loss of plasticity after three cycles on a single-screw extruder set at 102 rpm and with temperatures ranging from 220 to 290°C. A reduction of the elongation at break from more than 100% for vPET to 6% was observed, along with a tensile strength reduction from 63 to 52-55 MPa.

Some authors such as Frouchini et al. [14] reported contrary observations. On their study, even with a considerable molar mass decrease, the toughness modification was within the measurement error. Celik et al. [24] compared different commercially available PET recyclates and also showed that a differentiation between virgin (v) and recycled (r) PET was actually not possible in terms of mechanical characterization, since the vPET properties are already very broad.

Even though the embrittlement of PET materials after reprocessing is often described in literature, the scientific community has not yet reached an unanimity on its relationship with the structural modifications. Other aspects such as the physical aging, characteristic of a local densification of the amorphous phase over time, can also have a great effect on the embrittlement of glassy polymers [25–27]. To the best of our knowledge, the effect of physical aging on PET is not well understood.

In this context, the aim of this work is to examine the effect of several extrusion cycles on the mechanical response of a physically aged PET. Considering the physical aging for mechanical testing can give a more accurate characterization of the final properties of a product, when it has reached a stable state. By carefully controlling the preparation and the used PET grade, the structural modifications will be studied in terms of molar mass, thermal behavior, crystallization kinetics and color changes. The processing evolution and the rheological response will also be investigated in this non-formulated PET. Afterwards, without increasing the recyclates viscosity by a further post-condensation step, both tensile test and impact resistance will be studied. A correlation between the several observations should allow an accurate understanding of the different effects of structural changes in the mechanical response of a rPET. Establishing these connections can help reducing the technical challenges for PET recycling and expand its possibilities.

2 Materials and processing

2.1 Materials and reagents

A bottle-grade PET pellets of intrinsic viscosity (IV) $[\eta] = 0.88$ dL/g was purchased from Far Eastern New Century Corporation and named vPET for "virgin PET". Prior to every processing, PET pellets were dried at 140 °C for 4h. Then, during the cooling down to 50 °C, the vacuum was preserved. Residual humidity was confirmed using the calcium hydride method (DIN EN ISO 15512:2019) with Brabender Aquatrac-V (see evolution of the residual humidity as a function of the duration of exposure in Figure S1 in Supporting Information). For the dynamic rheological measurements, pellets were kept inside the rheometer chamber at 160 °C with a nitrogen flow of 2 L/min for 30 min.

For structural analysis, 1,1,1,3,3,3-Hexafluoro-2-propanol (≥ 99, 8% HFIP) and phenol/1,2-dichlorobenzene mixture (v:v 1:1) were purchased from Sigma Aldrich.

2.2 Materials processing

Mechanical recycling was simulated at a laboratory scale with successive extrusion cycles. A co-rotating twin-screw extruder (Haake Rheomex PTW 40 L/D, D=16 mm), with nine heating zones, was used (see Figure 1). The hopper was heated at 95 °C for avoiding humidity on pellets. The temperature profile from the feeder to the die was 285 (x3), 275, 270 °C (x6). The screw profile was composed of transport elements (2D-x4; 1D-x28) and 17 kneading elements (0° or 90° angles). The rotational speed was set at 320 rpm. The extrudate strand was pulled in a constant speed through a pelletizer after water quenching for rapid cooling. The recycled samples were named "rPET-Cx", where *Cx* represents the number of extrusions followed. After drying, part of the obtained pellets was fed into an injection molding press while the rest was used for the following extrusion cycle.

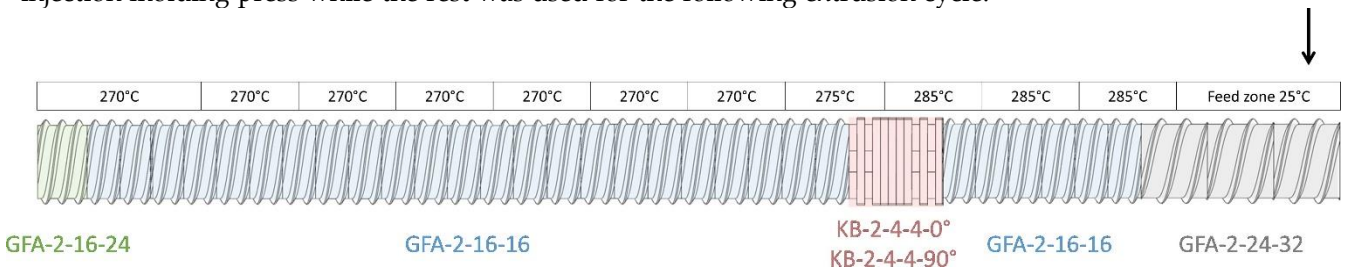

Figure 1: Schematic representation of screw profile used for this study.

Injection molding (Alecop Babyplast 6/12) was used for the preparation of mechanical test specimens. The screw rotation was set at 130 rpm and the temperature profile was 290, 290, 285 °C (two heating zones and the nozzle respectively). Samples were kept in a cold mold (20 °C) during 12 s for limiting their crystallization.

A schematic representation of the mechanical recycling simulation is available in Figure 2.

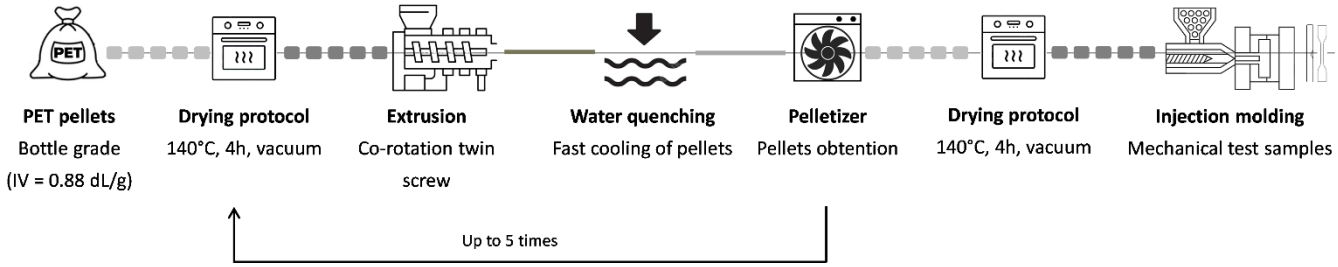

Figure 2: Schematic representation of the mechanical recycling cycles.

The recyclates were analyzed in terms of molar mass, acid content, color changes, thermal, and rheological behavior.

2.3 Methods of characterization

2.3.1 Size extrusion chromatography (SEC)

The molar mass distribution was determined by SEC Waters Acquity APCWyatt with a multiple detection system (viscosimeter, refractometer and multi-angle light scattering MALS set at 35 °C) and composed of four columns for optimum separation. Samples of around 10 g/L were prepared on HFIP and were filtered with a syringe filter CHROMAFIL Xtra PA-45/25, pore size 0.45 µm before injecting 20 µL (flow rate of 0.3 mL/min). The concentration was calculated with the refractometer and compared to the experimental value during the sample preparation. A mass recovery can be measured by a ratio between these two values.

The SEC-MALS-IV detectors allowed the determination of the branching ratio, thanks to Zimm-Stockmayer equation [28]:

$$g' = \left(\frac{[\eta]_{Mbranched}}{[\eta]_{Mlinear}}\right)^{\varepsilon} \quad (1)$$

where $[\eta]_{Mbranched}$ is the intrinsic viscosity of branched chains and $[\eta]_{Mlinear}$ of the linear ones, used as a reference (in our case vPET). ε is usually between 0.5 to 1.5 for, respectively, low or high branching. For PET, the chosen value was ε = 0.8 as it is considered a medium branching system [29].

2.3.2 Intrinsic viscosity (IV)

The IV was determined at 25 °C. Samples were prepared in a phenol/1,2-dichlorobenzene mixture at a concentration of around 5 g/L. The dissolution was done at 130 °C for 30 to 60 minutes in average. A filtration (syringe filter CHROMAFIL Xtra PA-45/25, pore size 0.45 µm) was done before the injection of 15 mL in a Ubbelohde viscometer

(Merck KGaA Darmstadt, Germany). IV was calculated from Ciuta et al. [30] equation (2):

$$IV = \lim_{C \to 0} \left(\frac{\frac{t - t_0}{t_0}}{C} \right) = \frac{\left(2 \times \left(\left(\frac{t - t_0}{t_0} \right) - \ln \left(\frac{t}{t_0} \right) \right) \right)^{\frac{1}{2}}}{C} \qquad (2)$$

where t_0 is the elution time of the solvent, t is the elution time of the solution containing the sample, and C is the concentration of the sample in the solvent.

2.3.3 Acid content

The carboxylic end-groups determination was performed by an external laboratory Indorama Ventures Fibers Germany GmbH laboratory at 80 °C according to ASTM D 7409 - 07. The acid concentration is given by an average of two measurements with a potentiometric titration method.

2.3.4 Dynamic rheology

Rheological properties were studied with a stress-controlled rotation rheometer DHR-2 from TA Instruments. Measurements were done at 280 °C after the drying of the pellets as indicated in subsection 2.1 with a 25 mm steel parallel plate and 1 mm gap. The linear viscoelastic region was measured with a amplitude sweep with an oscillation strain ranging from 10^{-3} to 10 and a defined angular frequency of 1 rad/s. The viscoelastic parameters (G', G'', η^*) were determined thanks to a frequency sweep from 100 to 0.1 rad/s and a controlled strain of 0.2.

2.3.5 Optical measurements

The CIE $L^*a^*b^*$ and the yellowness index (according to ASTM E313) were measured on injected specimens with X-RITE SP60 series spectrophotometer. The total color change in relation to the virgin material was calculated with the following equation 3, as suggested by Pinter et al. [31]:

$$\Delta E = \sqrt{(\Delta L^*)^2 + (\Delta a^*)^2 + (\Delta b^*)^2} \qquad (3)$$

with L^* for lightness, a^* for green to red and b^* for yellow to blue axis.

2.3.6 Thermal analysis

Differential scanning calorimetry DSC Q1000 from TA Instruments with a cooling system was used to measure the thermal transitions of PET pellets and injected objects. The sample of around 10 mg was introduced in a sealed aluminum pan. Non-isothermal measurements were done under nitrogen flow (25 mL/min) with a heating rate of

10 °C/min from 30 to 300 °C. A first heating was done to erase the processing history before cooling and re-heating again. Samples were kept for three minutes on each temperature plateau. Three analyses were done for each material.

Isothermal experiments were done to measure the crystallization kinetics on the same DSC equipment. Under nitrogen atmosphere (25 mL/min), samples were heated at 10 °C/min at 300 °C and kept at that temperature for three minutes. A cooling (20 °C/min) allowed to reach the isothermal temperature ranging from 205 to 235 °C for different durations. Although this is not the most common method for isothermal crystallization studies, for which the cooling prior to the isotherm is more abrupt, these conditions were selected for practical reasons, and the data will be analyzed in a comparative manner. The same heating and cooling cycle as the non-isothermal measurement were done at the end of the isothermal crystallization. No prior drying was done before DSC analysis.

The degree of crystallinity was measured according to the equation:

$$\chi_c = 100 \times \left(\frac{\Delta H_m - \Delta H_{cc}}{\Delta H_m^{th}}\right) \; with \; \Delta H_m^{th} = 135.8 J/g \; [32] \tag{4}$$

where ΔH_m and ΔH_{cc} represent, respectively, the melting and cold crystallization enthalpy measured from DSC data obtained in heating runs.

The crystalline phase growth was observed using an optical microscope equipped with crossed polarizers and a waveplate. Specimens were placed between two microscope slides inside a heating stage where a rapid cooling to the isothermal temperature was done. Pictures were taken every 30 s for different isothermal durations.

Thermogravimetry analysis (TGA) was done with a TGA/DSC 1 Star^e System from Mettler Toledo under air flow (25 mL/min). Aluminum crucibles of 100 µL (1/8 ME-51119872) were used without sealing with around 10 to 20 mg (1 pellet). Samples were heated without prior drying from 30 to 600°C at 10 °C/min.

2.3.7 Mechanical characterization

Uniaxial tensile tests were performed in a universal testing machine Zwick Roell Z050 at 5 mm/min. For each reference, five injected dumbbell shaped samples (ISO 527-2, type 5a) were used. An accelerated physical aging in an oven set at 50 °C for 7 days was done before testing. Stress-strain curves were obtained and parameters such as Young's modulus (E), yield strength (σ_e) and elongation at break (ε_{break}) were extracted. An extensometer was used only for the E measurement.

Impact tests were performed with an Instron CEAST 9050 machine (5,5 J pendulum according to the standard ASTM D256) in Izod mode. Notches (45° single V-notch with 0.25 mm radius, accordingly to NF EN ISO 180) were machined with an Instron CEAST AN50 on the injected molded bars (10x40x30 mm).

3 Results and discussion

3.1 Impact of the processing cycles on the rPET molar mass

PET was reprocessed in an extrusion line up to five times with a pre-dyring step before each cycle. As a reminder, in order to achieve a successful recycling of PET, certain minimum technical requirements should be respected specially in what concerns the water content in the pellets [9]. Therefore, a prior validation of the drying conditions was thoroughly conducted. The residual humidity after the preparation step was confirmed at around 50 ppm, remaining lower than 200 ppm as recommended [10], at least for 2h30 of processing. The drying protocol also allowed an increase of PET crystallinity (up to around $\chi_c = 35\%$), reducing the water absorption and therefore degradation, as mainly the amorphous phase is concerned by the hydrolysis process [33].

The recorded torque on the screws and the average flow rate are reported in Table 1. The decrease in torque with the number of reprocessing (average values), from 85 Nm for vPET down to 53 Nm for rPET-C5, is related to a loss of viscosity probably due to chain scission reactions [16]. One direct result of this degradation was a processability instability, noticeably worsen with the increasing number of cycles. The extrudate became thinner and more fragile to the pelletizer pulling, even with an increasing flow rate from initially 0.84 to 1.44 kg/h at the last cycle (the unexpected torque evolution with recycling can also be related to these varying processing parameters). Several breaks and extrudate elongation could be observed during the recycling process, inducing a heterogeneous pellet dimension. Other authors who studied a similar recycling simulation, have also experienced this kind of processing difficulty [20].

Table 1: Extrusion parameters after each recycling cycle.

Sample	Average torque (Nm)	Average flow rate (kg/h)
vPET	85	0.84
rPET-C1	73	0.69
rPET-C2	54	0.81
rPET-C3	59	1.10
rPET-C4	48	1.10
rPET-C5	53	1.44

SEC, IV and acid titration data are available in Table 2 and Figure 3. A significant molar mass decrease can be observed after each extrusion cycle and which tends towards a plateau after four cycles. During processing, PET is exposed to high temperatures and significant shearing that is known to cause the material degradation even if well dried [19,34,35]. These severe experimental conditions cause thermal and thermal-oxidative reactions responsible for the material chain scission. A slight reduction of the polydispersity was also observed by other authors [19,36]. These phenomena lead to an increase of the acid content which can be attributed to the presence of carboxyl end-groups from thermal and hydrolytic mechanisms [36, 37].

Although the IV values were not determined for all samples because of time constrains, its reduction between the first and fifth recycling cycles leads us to think that no cross-linking took place during this process, not observed either in other works [12,16]. The HFIP solubility of all samples, with a constant mass recovery in the range of 85 to 95%, also supports this hypothesis. The chromatography depicted in Figure 3 indicates a symmetrical peak, with no second populations in a Gaussian-like distribution. The signal at around 10.8 min is from the HFIP solvent and at 11.5 min from cyclic oligomers from the polymerization. Usually present at levels of 2-3% [10], these oligomers concentration seems to have remained stable during our recycling process. Hence, the limitation of five on the maximum number of extrusions that could be performed was probably a result of the low viscosity of the samples and not branching or gelation as reported by other authors [12]. In Assadi et al. [12] work, for instance, no SEC data are available over the third cycle because of observed insolubility related to this gelation process at the fourth extrusion cycle.

Table 2: Average molar mass in weight (Mw), in number (Mn), polydispersity index ($Đ$) obtained by SEC analysis (HFIP as solvent) experiment of PET pellets. The intrinsic viscosity values of some of the samples were not analyzed due to time constraints and prioritization of other key experiments.

Sample	vPET	rPET-C1	rPET-C3	rPET-C4	rPET-C5
Mn (kg/mol) - ± 10 %	29.9	27.0	20.6	20.4	21.6
Mw (kg/mol) - ± 10 %	54.4	43.5	36.9	34.0	33.4
Đ	1.8	1.6	1.8	1.7	1.5
IV (dL/g)	0.88	0.72	x	x	0.61
COOH (mmol/kg)	24.9	31.4	x	x	48.1

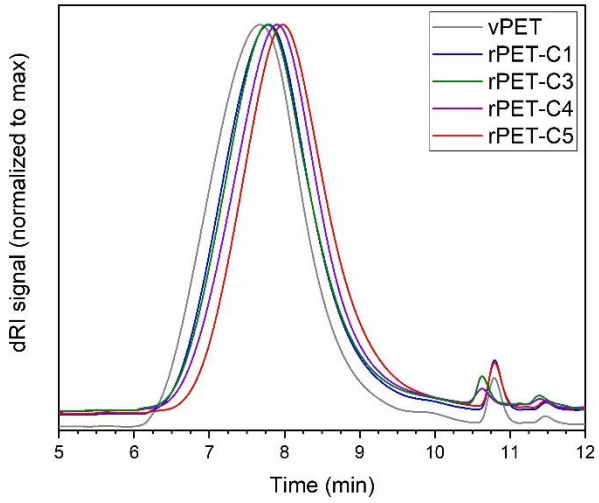

Figure 3: Light scattering signal as a function of the elution time in a HFIP SEC experiment.

Using the viscosimeter detector, a throughout study of the possible branching on the recycled samples was done. Figure 4(a) show the relationship between IV and Mw determined thanks to the SEC-MALS-IV stack in HFIP. The Mark-Houwink-Sakurada parameters, that determine the chain conformation, did not vary between the cycles. They stayed constant at 0.7, being characteristic of a flexible chain. The slight deviation in the range corresponding to the

high molar mass, in Figure 4(a), can be related to a possible branching of chains, which is more important after five extrusions.

Indeed, the results of the branching ratio (see Figure 4(b)) showed that after one cycle, only 2.2% of the whole molar mass range was branched, while 4.5% is reached in the case of rPET-C5. However, it is important to notice that this phenomenon concerns only a small number of chains, mainly in a molar mass range above 80 kg/mol, which represents less than 5 % of the total number of chains in the sample (see cumulative weight fraction curves in Figure S2 in Supporting Information). Additionally, the limited branching did not result in a substantial alteration in the already short hydrodynamic radius, not detectable by our measurement methods.

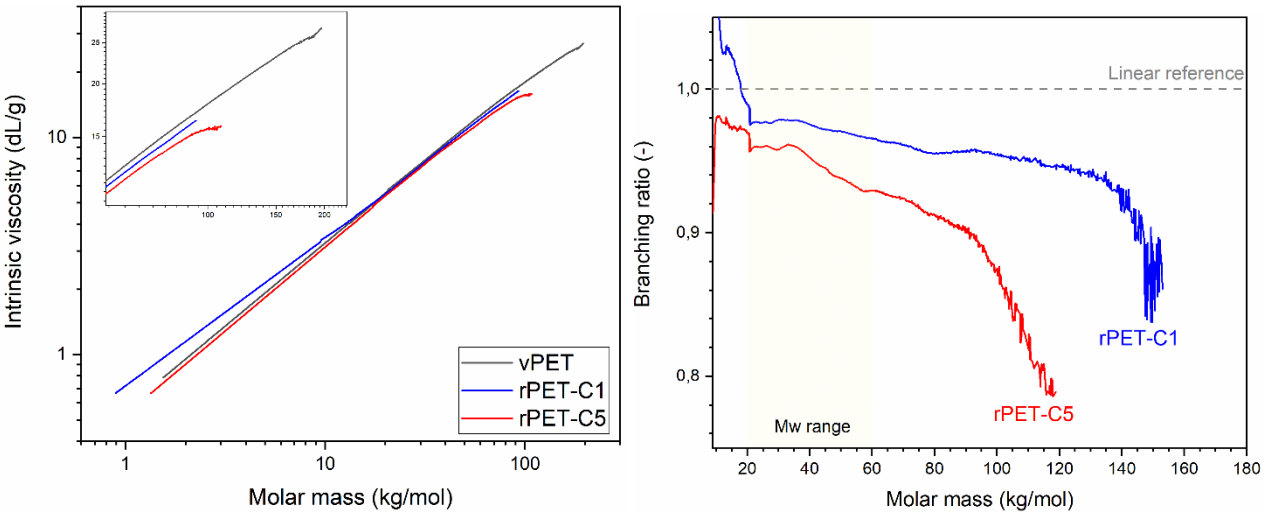

Figure 4: SEC-MALS-IV study. (a) Mark-Houwink-Sakurada curves, log plot. (b) Branching ratio as a function of the molar mass.

The recyclates response on an oscillatory rheological measurement is shown in Figure 5(a). The data was performed in the linear viscoelastic regime. Parameters such as the storage and loss moduli determined as a function of the angular frequency can fully describe the material response. The reduction in the loss modulus with the number of recycling cycles can be linked to the processing-induced chain scissions. The loss of Mw, and consequently of the viscosity, can also be followed in Figure 5(b). The viscosity decreases of a factor 4.9 between virgin and rPET-C5. Moreover, the increase in the elastic response at low frequencies, especially for five-time reprocessed PET, tends to confirm the observed branching in SEC. As a reminder, branching in PET can be associated with thermo-oxidative degradations in presence of low partial pressure of oxygen. Indeed, the formation and combination of radicals on the alkyl portion of the polyester structure can induce branching and, if severe, crosslinking [16, 34].

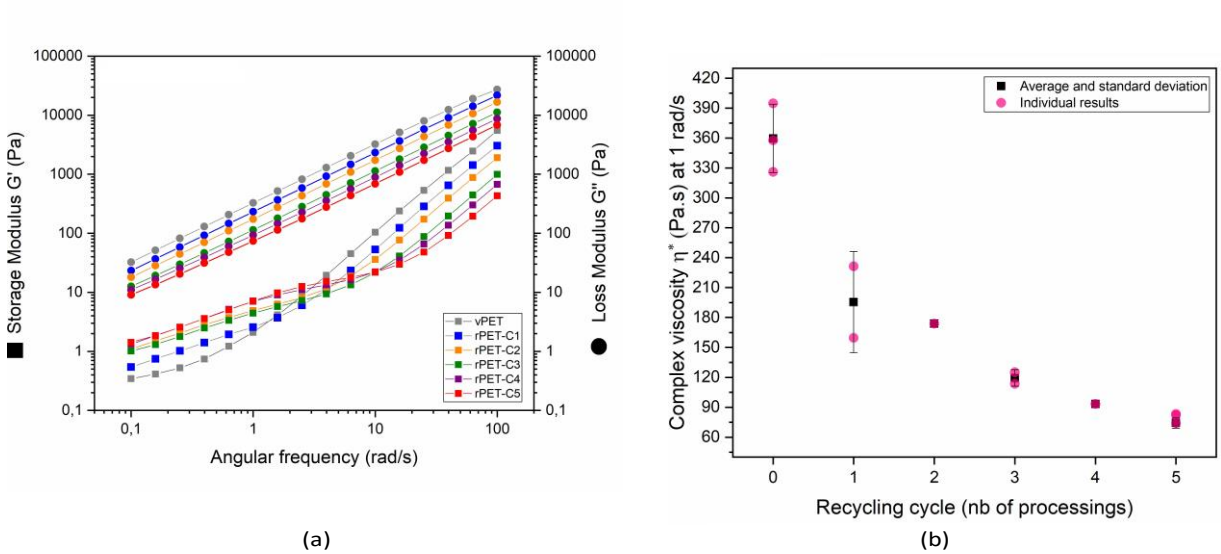

(a) (b)

Figure 5: Frequency sweep under nitrogen flow et 280°C. (a) Evolution of storage and loss moduli as a function of the angular frequency. (b) Newtonian viscosity at 1 rad/s.

Once a complete study of the morphology of extruded pellets was done, the effect of the injection molding process was studied in terms of chain scission. Table 3 contains the results of SEC measurements after the injection of the produced pellets.

Table 3: Average molar mass in weight (Mw), in number (Mn), polydispersity index ($Đ$) obtained by SEC analysis (HFIP) of a PET tensile test samples core (injected pellets).

Injected specimens	vPET	rPET-C1	rPET-C3	rPET-C5
Mn (kg/mol) - ± 10 %	23.5	20.6	17.5	17.0
Mw (kg/mol) - ± 10 %	38.6	35.5	31.3	27.8
Đ	1.6	1.7	1.8	1.6

Such as all processing methods for polymers, high shearing at high temperatures lead to a degradation of the material. After injection, all samples have a reduction in their Mw, of 29% loss for vPET and around 16% for rPET. It is important to keep in mind that the percentage of loss reduces progressively over the cycles to reach a plateau level, where chains are too short to be further degraded [15, 17].

In terms of chain cleavages, one cycle of injection molding is more severe than one extrusion step. Although the same temperature range (260 to 275 °C and same cycle duration (around 1 minute between dosing and injecting) are used. The more pronounced decrease in molar mass with injection molding technique when compared to extrusion has been observed by other authors [38]. Although the same temperature range (260 to 275 °C) and same cycle duration (around 1 minute between dosing and injecting) are used for both techniques, during injection-molding, the polymer is exposed to higher pressures (around 1000 bar) and shear rates (up to 10^6 s^{-1}) [38, 39].

3.2 Aspect modification

The aspect modification of PET after recycling was measured using a spectrophotometer. Table 4 contains the data for all samples. As can be seen, both a^* and b^* parameters increase with the number of processing while L^* values decreases. The total color change ΔE and the Yi were used to compare the overall aspect modification (see Equation 3 and Figure 6(a)) [31]. A significant and constant increase can be seen after each cycle. In terms of Yi, an increase between 4-15% is observed after each extrusion, evolving from from 13.9 for vPET to 27.1 for rPET-C5. This difference in terms of yellowing is even visible with the naked eye (see Figure 6(b)), as the delta in the b^* axis exceeds 2 [40]. The ΔE evolution is also pronounced, reaching 8.3 units after five successive cycles. The lightness, represented by L^*, reduces constantly with recycling from 84.6 to 79.0. Interestingly, rPET kept a perfect transparency for all samples.

Table 4: Data from the spectrophotometer analysis. The standard deviation is done over three measurements for each sample.

Extrusion	CIE L^* a^* b^* data				Color change
Cycle	L^*	a^*	b^*	Yi	ΔE
vPET	84.6 ± 0.5	-0.63 ± 0.04	7.0 ± 0.4	13.9 ± 0.8	x
rPET-C1	83.6 ± 0.1	-0.52 ± 0.02	8.3 ± 0.3	16.6 ± 0.8	1.7
rPET-C2	83.2 ± 0.6	-0.41 ± 0.06	8.6 ± 0.3	17.3 ± 0.8	2.2
rPET-C3	81.2 ± 0.8	-0.28 ± 0.01	9.7 ± 0.1	20.0 ± 0.8	4.4
rPET-C4	80.8 ± 0.1	-0.30 ± 0.03	11.5 ± 0.0	23.6 ± 0.8	5.9
rPET-C5	79.0 ± 0.2	-0.09 ± 0.03	13.0 ± 0.9	27.1 ± 0.7	8.3

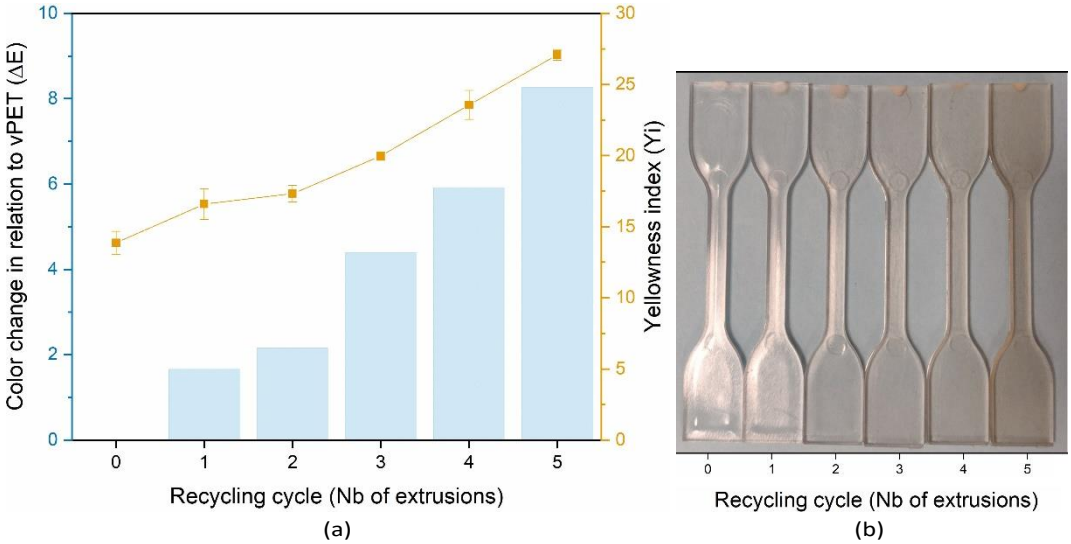

Figure 6: (a) Total color change (ΔE) and yellowness index (Yi) as a function of the number of recycling cycle. Picture of injected tensile specimens showing the visual yellowing and transparency of vPET and rPET.

PET yellowing and color change can be used as makers for degradation mechanisms, especially thermally and oxygen activated ones, indicating the presence of chromophoric by-products [17]. The main species responsible for this color modification seem to be polyenes, polyenaldehydes, and quinoid types structures (see Figure 7 and

Figure 8) [10,41–45]. The yellowing is faster in presence of oxygen, that will favor the formation of conjugated aromatics and quinoid species. Residues from catalysts used during synthesis tend to accelerate yellowing too [37]. Moreover, in bottle applications, for instance, the presence of other materials such as polyamides, used as a barrier layer, can further contribute to yellowing via other mechanisms [42]. In the present work, the chemical species responsible of yellowing were not quantified, however it was a simple way of evaluating the state of degradation of recycled samples.

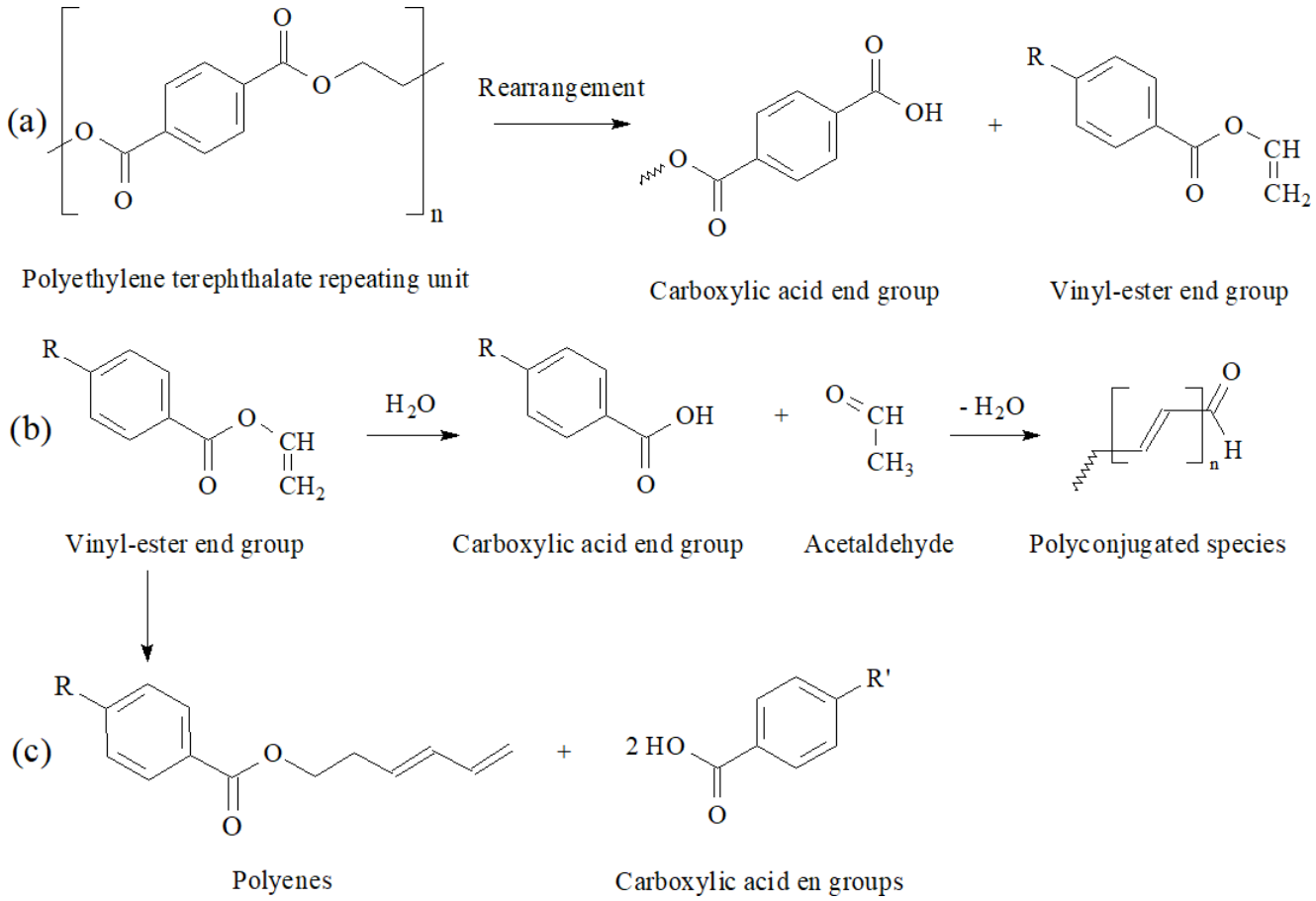

Figure 7: Simplified reaction mechanisms for the formation of chromophores in PET. (a) Thermal degradation for the formation of carboxylic acid and vinyl-ester en groups [37]. (b) Polyconjugated species from aldol condensation of acetaldehyde [10]. (c) Formation of polyenes from polymerization of vinyl-ester and elimination of carboxylic acids [44, 45]. Adapted with permission from [44]. Copyright 1995, Elsevier.

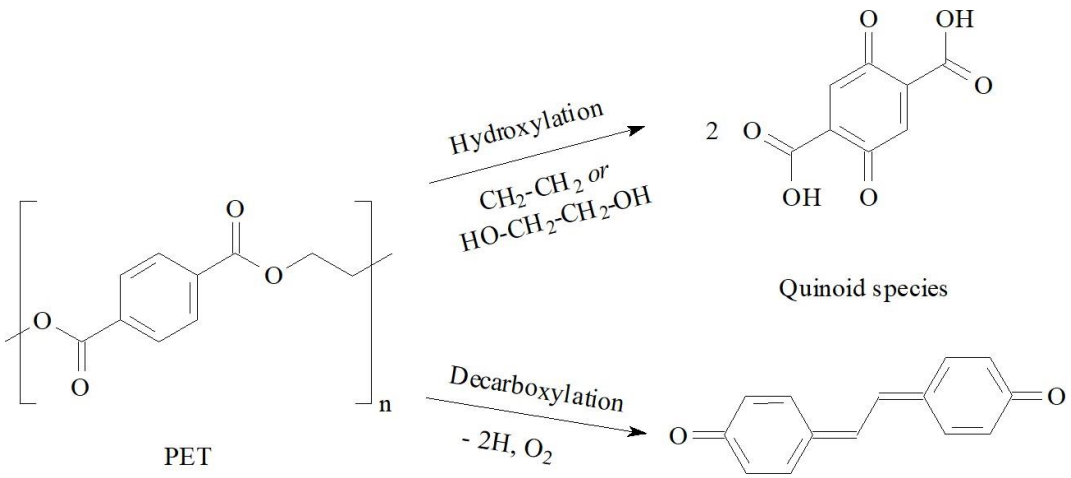

Figure 8: Simplified mechanisms for the formation of chromophoric quinoid species in presence of oxygen from PET structure.

After recycling, similar aspect modifications have been described in literature, confirming the increasing degradation with processing [17,31]. For the re-use of a post-consumer PET, the *Yi* should not exceed 20 [9]. In our case, without a further addition of anti-yellowing agents, a maximum of only two recycling cycles would be acceptable. Other authors claim that a quality parameter for PET bottles chips is a $b^* < 1$ [40], meaning that even for vPET, additives would have to be added. In terms of lightness, typical industrial specifications for PET bottles if between 85 to 90 units [46], higher than almost all our values.

3.3 Thermal and crystallization behavior

TGA analysis

The thermal stability of recycled pellets was studied using TGA analysis under air. The degradation of PET is expected in two steps: one at 300-350 °C from the shortening of longer chains, and a second at around 560 °C from the thermo-oxydative degradation of the formed small fragments [47, 48].

The TGA data are depicted in Figure S3 and Table S2 in Supporting information. As anticipated, the degradation process in two distinct steps was indeed confirmed for all samples. A first and sharp loss (average of 86%) started at around 405 °C, with a temperature peak at around 430 °C. The second loss of around 13.5% started at 548 °C with a peak at 571 °C. No significant differences were observed between vPET and rPET. Under nitrogen, the degradation occurs in only one step starting at around 415 °C and reaching a peak at 435 °C with 88% weight loss.

Non-isothermal DSC analysis

The effect of processing cycles on PET's thermal transitions was studied via DSC thermograms. They are available in Figure 9 and presented in Tables 5 and 6. Parameters such as crystallization and melting temperatures (*Tc* or *Tm* respectively), enthalpies (ΔH_c and ΔH_m from melting or crystallization respectively) and crystallinity degree (χ_c) can give information about the material microstructure.

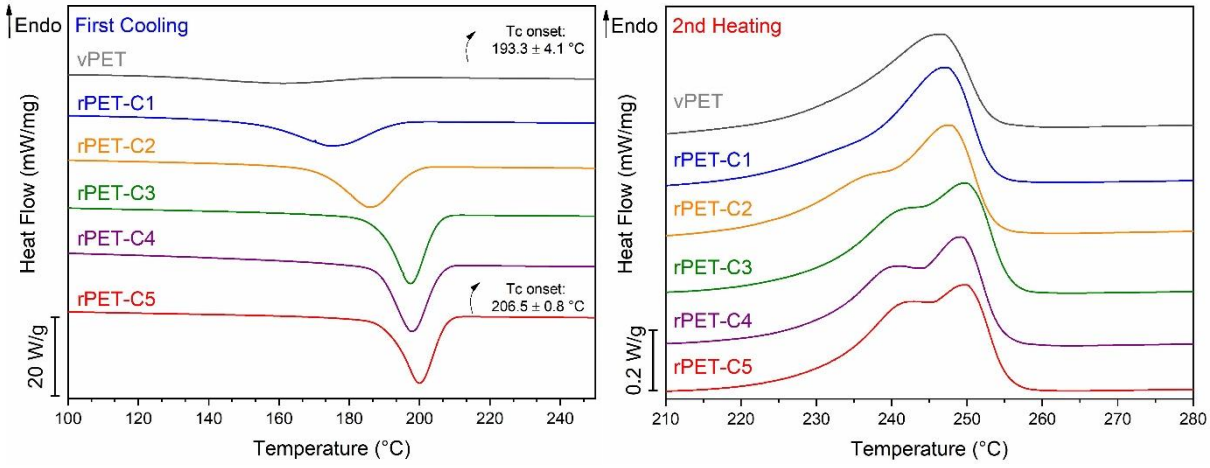

Figure 9: DSC thermograms for virgin and reprocesses PET pellets recorded at 10°C/min. (a) First cooling from the melt. (b) Second heating, zoom of the melting area.

Table 5: Thermal properties of PET obtained from DSC cooling from the melt, available in Figure 9(a).

Sample	Pellets first cooling - 300°C to 30°C - 10°C/min		
	Tc onset (°C)	Tc peak (°C)	χ (%)
vPET	193.3 ± 4.1	161.6 ± 2.4	19.6 ± 1.4
rPET-C1	190.2 ± 4.7	169.1 ± 9.0	24.7 ± 6.6
rPET-C2	200.2 ± 1.5	188.5 ± 2.6	32.0 ± 0.5
rPET-C3	204.9 ± 0.2	197.3 ± 0.2	33.8 ± 0.9
rPET-C4	206.0 ± 0.2	198.1 ± 0.7	34.2 ± 1.2
rPET-C5	206.5 ± 0.8	198.6 ± 1.2	32.9 ± 1.5

A first heating curve was used for erasing the processing history of studied pellets. By studying the cooling curves available in Figure 9(a), it can be seen that the crystallization transition is shifted to higher temperatures and seems to be sharper with the increasing number of processing. Indeed, a wide crystallization peak at low temperatures is characteristics of a slow crystallization from high molecular weight polymers such as the used reference [20]. The rPET-C5 pellets start crystallizing at a temperature more than 10 °C higher than the virgin one. The crystallization temperature peak is even more affected in comparison with vPET, with a delta of 8 °C after a first extrusion and evolving to 37 °C after five cycles of extrusion. The crystallinity is also deeply affected, increasing constantly until around 34 %. In other terms, the more the pellets are recycled, the earlier (shift to higher temperatures) and faster (sharper transition) is the crystallization.

Table 6: Thermal properties of PET from DSC second heating available in Figure 9(b).

Sample	Pellets Second heating - 30°C to 300°C - 10°C/min				
	Tg midset (°C)	ΔCp (J/(g.°C))	Tm onset (°C)	Tm peak (°C)	χ (%)
vPET	80.7 ± 0.5	0.261 ± 0.03	232.4 ± 0.7	248.5 ± 0.4	18.6 ± 3.4
rPET-C1	80.6 ± 0.2	0.166 ± 0.01	232.6 ± 0.4	247.2 ± 0.3	31.3 ± 0.5
rPET-C2	80.6 ± 1.1	0.158 ± 0.01	233.2 ± 0.3	248.3 ± 0.6	33.5 ± 0.9
rPET-C3	79.5 ± 0.4	0.149 ± 0.03	227.4 ± 0.2	249.3 ± 0.4	36.8 ± 0.7
rPET-C4	80.3 ± 0.5	0.161 ± 0.01	232.3 ± 3.7	249.3 ± 0.3	36.8 ± 1.7
rPET-C5	80.7 ± 1.3	0.150 ± 0.02	228.9 ± 0.7	249.4 ± 0.5	35.6 ± 2.5

Figure 9(b) displays the second heating curves, where the presence of a bimodal melting peak becomes clearer with the increasing number of recycling. The first peak amplitude increases after each cycle, to the detriment of the second peak. Another observation is a slight shift of the *Tm* from 247.2 °C to 249.4 °C between rPET-C1 and rPET-C5. A crystallinity increase is visible and a little more marked than this obtained from the cooling curves, reaching an average value of χ_c = 35%, almost twice more than vPET. The glass transition temperature (*Tg*) is not significantly affected, remaining at around 80 °C for all samples. Noteworthy, vPET pellets present a cold crystallization peak that is not present in the other cycles, explaining the lower value of χ_c for this sample (see Equation 3). This will also affect the heat capacity (ΔCp), higher for less crystalline samples.

The increase in the crystallinity after mechanically recycling PET has been described by several authors [13,17, 20, 48–50]. The explanation for this phenomenon is mostly related to the chain scission process and the presence of branching observed earlier. The shorten of the chain length caused by the different degradation mechanisms increased the chain mobility, favoring an overall reorganization in the material [13,50,51]. The presence of shorter chains, which can easily fit among larger ones, can explain the overall crystallinity increase [13,52]. These segments of chains may also favor the nuclei presence and number [53]. Another possible explanation is the presence of impurities from the extrusion cycles that may act as nucleating agents [17,50]. Finally, the enrichment in the trans conformation of PET was also related to this increasing crystallinity in some papers and can be another explanation in our case [20].

The melting curves in Figure 6(b) also suggest a heterogeneity of the chain length in the polymer. The appearance of a second *Tm* is associated with thinner lamellae population, that can be due to the chemical modification during extrusion leading to chain shortening [13] or branching.

Microstructural modification can have a direct effect on the mechanical properties, and are often associated with the embrittlement of the material [11,13]. In order to minimize that effect and limit the crystallization for the preparation of mechanical test specimens, the mold temperature was set at 20 °C in the injection molding press. However, the strong orientation of chains during this process will inevitably engender an increase in the crystallinity of the samples [46, 50]. this process is also responsible for inducing a further degradation as seen in Section 3.1.

Table 7 shows that even after quenching in water at the extruder exit, or in a cold mold, samples that have been reprocessed tend to crystallize more and more. The crystallinity is still relatively low in all cases.

Table 7: Crystallization data from first heating curves on DSC for pellets and injected samples.

Sample	First Heating 30 °C to 300 °C, 10 °C/min					
	Extrusion (pellets)			Injection molding (tensile specimens)		
	ΔH cc (J/g)	ΔH m (J/g)	χ (%)	ΔH cc (J/g)	ΔH m (J/g)	χ (%)
vPET	x	64.6 ± 0.4	47.5 ± 0.3	21.0 ± 1.0	39.3 ± 0.0	13.5 ± 0.8
rPET-C1	34.0 ± 1.1	40.0 ± 2.0	4.4 ± 1.4	20.6 ± 2.8	41.3 ± 2.1	15.2 ± 1.3
rPET-C2	30.9 ± 3.3	41.6 ± 0.9	7.9 ± 3.0	21.1 ± 1.4	41.1 ± 2.4	14.7 ± 0.8
rPET-C3	33.8 ± 0.2	44.6 ± 0.6	7.9 ± 0.3	21.8 ± 1.8	41.6 ± 2.3	14.6 ± 0.6
rPET-C4	33.6 ± 1.1	45.0 ± 1.0	8.4 ± 0.2	23.0 ± 2.5	45.3 ± 1.9	16.4 ± 3.3
rPET-C5	27.8 ± 2.6	45.1 ± 0.9	12.7 ± 1.3	22.0 ± 1.7	44.0 ± 1.3	17.8 ± 0.0

In Figure 10, the *Tc* from cooling of molten pellets and injected samples are compared. As expected, injected samples have a constant increase of their *Tc*, indicating an increase of crystallization kinetics, as observed in other articles [50]. The crystallinity degree reaches a plateau of around χ_c=31% for all samples with at least one extrusion. Once again, as discussed before, this can be a result of both the higher mobility induced by chain scission and the orientation of chains provided by this processing. The presence of bimodal melting peak was also observed for injected specimens, suggesting that the heterogeneity of the chain lengths, and/or the presence of branching, is still visible. The nucleating effect brought by the increasing concentration of impurities from extrusion may play a role on this phenomenon.

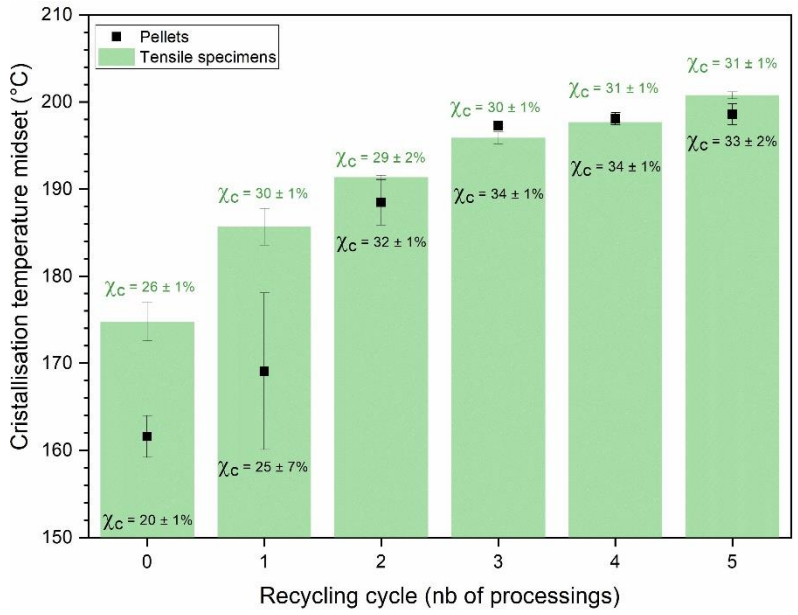

Figure 10: Evolution of the crystallization temperature (*Tc*) with the number of processing for pellets and tensile test samples. The crystallinity is also visible for pellets (in black) and for tensile specimens (in green). Data obtained from DSC curves from cooling.

Isothermal DSC

A complementary study was done by isothermal tests by DSC. Figure 11 shows the evolution of the crystallization kinetics with the number of recycling. Table 8 shows the obtained data from the melting endothermic. As can be seen, the more recycled sample, the shorter the crystallization duration, shifting the curves to lower crystallization times. The molar mass reduction can be at the origin of this phenomenon, even if the chain mobility is not the limiting factor at this temperature range. This observation confirms the increase in the crystallization rate for rPET, already established with dynamic curves (see Figure 6(a)). As the isothermal temperature increases, this phenomenon becomes even more predominant. The final crystallinity after isothermal tests in Table 8 varies from 30 to 55 % but start much earlier for recycled samples as expected.

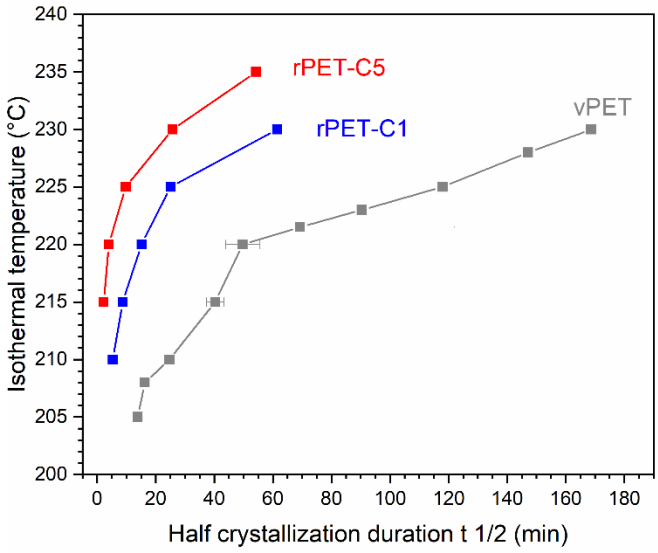

Figure 11: Recycling effect on crystallization kinetics via DSC. Isothermal temperature as a function of half crystallization time.

Table 8: Thermal properties data obtained after heating from the temperature of isothermal crystallization up to 300 °C at 10 °C/min by DSC.

Sample	Tiso (°C)	t start (min)	Tm peak (°C)	ΔH f (J/g)	χ (%)
vPET	**230**	**110**	**241.1**	**70**	**52**
	220	11	242.0	58	43
	210	**5**	**240.2**	**31**	**23**
rPET-C1	**230**	**19**	**254.9**	**30**	**42**
	220	4	250.1	51	38
	210	**1**	**245.6**	**39**	**56**
rPET-C5	230	9	253.5	53	39
	220	**3**	**252.3**	**62**	**46**
	210	0	250.7	60	44

In isothermal conditions, when no mechanical stress is applied to a crystallizing material from the molten state, spherulites can be formed, spreading at the expense of the still liquid region [10, 54, 55]. Their formation starts with the appearance of a nucleus that grows once a critical size is reached to form these spherical shapes. Their growth is limited by the contact with other growing spherulites, so the more is the nucleation, the smaller are the spherulites at the end of crystallization. Thanks to the birefringence nature of this crystalline phase, the spherulite growth can be followed by an optical microscopy equipped with crossed polarizers and a wave-plate.

Figure 11 shows the growth of these spherical structures in pellets and in injected specimens at 230 °C. This specific temperature was chosen as the best compromise between the samples, as the crystallization duration varied a lot between rPET and vPET. They allow a visual observation of the nucleating effect brought by successive reprocessing. In Figure 12(a), at almost the same duration, rPET-C5 nucleate faster than rPET-C1. On the contrary, after the same duration of 7 minutes, vPET did not show any sign of spherulite nuclei, starting to appear only after 15 minutes. After 30 minutes, vPET have bigger and less numerous spherulites that continue to grow. The observations were different for injected samples (see Figure 12(b)). As expected, the nucleation of all samples is increased, starting only a few minutes after the reaching of the isothermal temperature.

Thanks to a zoom in specific zones of these images (not showed in this article), the spherulite radius was measured over time, allowing the determination of their growth rate, which is the slope of the line presented in Figure 13. Noteworthy, the measured radius from the optical microscopy pictures concern only a thin layer trapped between two microscope slides (some particles can be hidden), and the contact with the surface can also favor the nucleation.

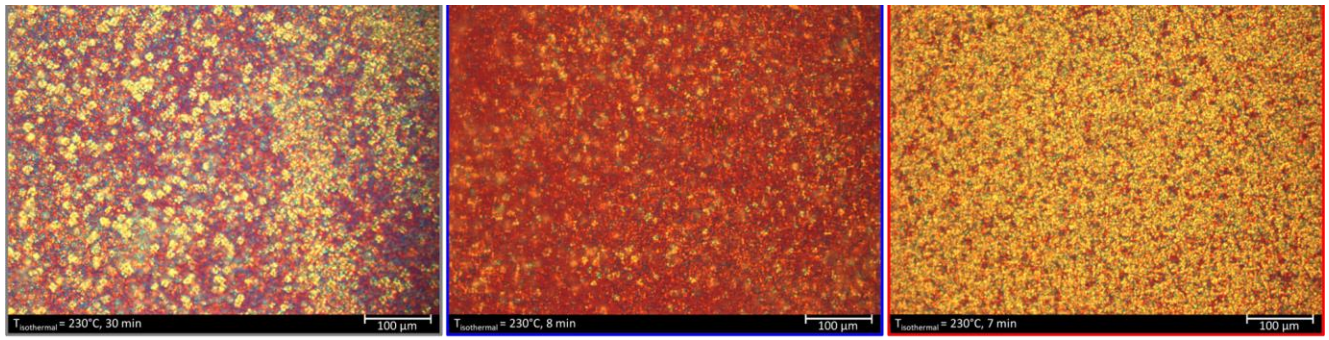

(a)

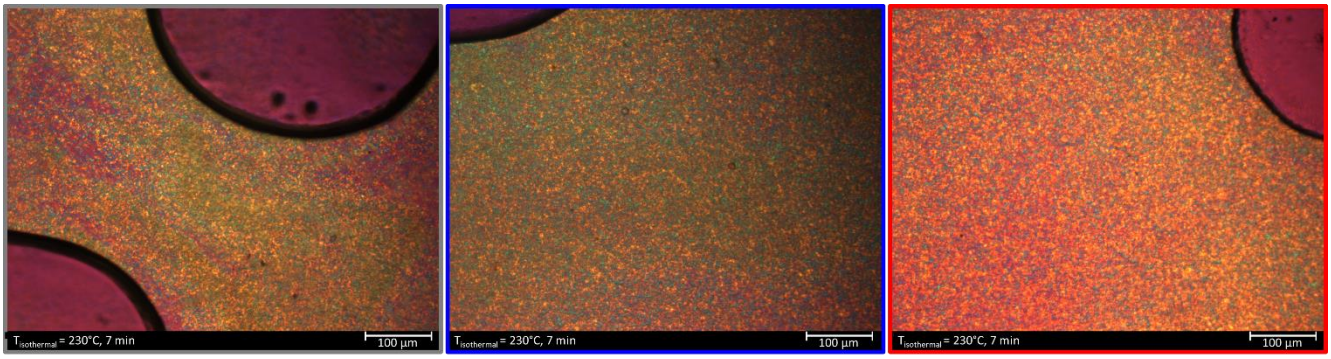

(b)

Figure 12: Isothermal crystallization at 230 °C for different durations. Pictures obtained with an optical microscopy with polarized light. (a) Extruded pellets of vPET (30 min), rPET-C1 (8 min) and rPET-C5 (7 min) from left to right. (b) Injected tensile specimens at 7 minutes of crystallization of vPET, rPET-C1 and rPET-C5 from left to right.

Anyhow, the results indicate that rPET has around three times faster spherulite growth when compared to the virgin material (equal to 0.48 µm/min), probably a result of the chain scission process. Samples reprocessed once or five times, have a similar crystalline phase kinetics as their growth rate is comparable, respectively at 1.26 and 1.76 µm/min. The observed branching in rPET-C5 tend to slow the growth rate, limiting the accelerating effect of a lower Mw and explaining the similitudes between rPET-C1 and rPET-C5. The increase in the overall crystallinity (see Table 7) is therefore related to the rate of nucleation. In other words, once the spherulites are formed, they grow at a similar rate but do not reach the same size. The final spherulite radius in Figure 13 was 18.9 µm for vPET while recycled one or five times reached respectively 17.1 and 11.6 µm in average. This study allowed, therefore, to quantify the nucleation differences that might explain some of the mechanical response. In literature, the impact strength is usually inversely proportional to the spherulite size [56,57]. The presence of an intercrystalline phase, connecting spherulites together, play also a role in increasing the mechanical strength of polymers [56].

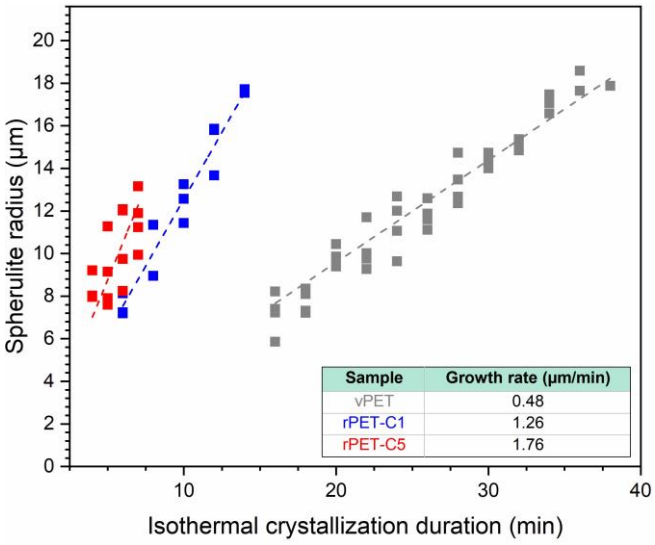

Figure 13: Evolution of spherulite radius of PET pellets, measured in zooms of the optical microscopy pictures in Figure 12(a), in chosen spots were the size of the spherulites was measurable. The growth rate was determined by the linear fitting of the data in dashed line.

3.4 Mechanical behavior

Uniaxial tensile tests

The stress-strain curves of vPET and rPET are available in Figure 14 and the corresponding data in Table 9. It can be noticed that the overall behavior in tensile test is similar for all samples. During testing, the necking went through the whole specimen before breaking. A stiffness increase was observed, with a variation in the Young's modulus from around 2310 MPa for vPET to 2500 MPa for rPET-C5. Other parameters such as the yield stress did not vary significantly, staying constant at σ_e=55 ± 1 MPa. The elongation at break stays very high, close to 500% for all samples. A slight decrease to ε_{break}=483% can be seen for the 5-time rPET, still characteristic of a ductile material.

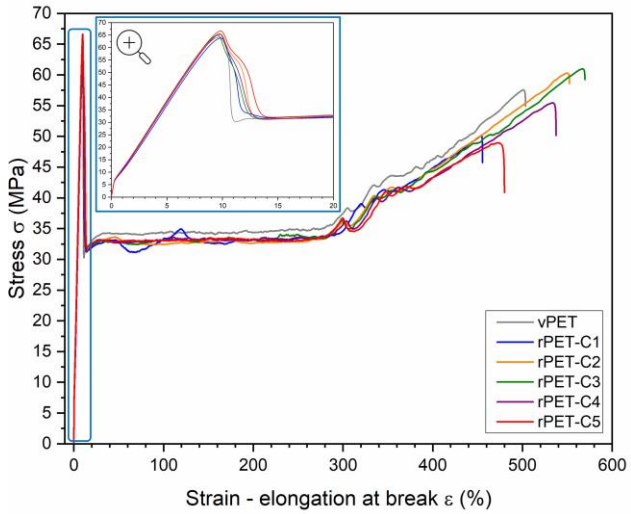

Figure 14: Strain-stress curves from uniaxial tensile testing after aging.

Table 9: Data from the strain-stress curves showing the Young's modulus (E), the yield strength (σ_e) and the elongation at break (ε_{break}).

Sample	Young's Module (MPa)	Yield strenght (MPa)	Elongation at break (%)
vPET	2246 ± 266	63 ± 1	499 ± 15
rPET- C1	2341 ± 172	64 ± 1	511 ± 49
rPET-C2	2320 ± 207	65 ± 1	509 ± 65
rPET-C3	2520 ± 98	65 ± 1	557 ± 11
rPET-C4	2626 ± 154	65 ± 1	549 ± 11
rPET-C5	2597 ± 127	65 ± 1	483 ± 2

In literature, a direct relationship between chain scission and a loss of mechanical properties is often described for polymers in general [51,58] and also for mechanically recycled PET [15,17–19]. But the results of our recycling process may witness of a more complex effect of microstructure changes in the final response of the material. This usual straightforward view for polymers overlooks the effect of processing and molar mass loss in the crystallization process [51]. Indeed, injection molding engendered a constant decrease of molar mass of the extrudate pellets. Therefore, by focusing only on this aspect, an increasing fragility would be expected in tensile tests such as observed in literature. However, chains scission, combined with impurities from processing, increased the crystallinity of the specimens from 14% to 18% in average (see Table 7). This would engender an opposite effect in glassy polymers, with a rigidification from the crystalline phase development at the expense of the amorphous phase that guarantees a ductility.

Thus, the overall modest modification in our case could be linked to the competition between these two mechanisms, even if the effect of crystallinity at temperatures below the *Tg* of the polymer has only a weak influence on the mechanical response. It is important to point out that the remaining ductility of these mostly amorphous samples allows us to assume that the critical molar mass Mc (usually given at Mc = 17 kg/mol) was not yet reached even after five recycling cycles. The PET chains are probably still entangled before testing as the

observed plastic deformation is associated with a disentanglement during uniaxial solicitation [51].

The concept of Mc has also been used in other works to explain the remaining ductility of PET after recycling [59], although its exact value is not perfectly clear in literature (a variation from 10 to 18 kg/mol is also described [12, 60–62]). On the other hand, the most common effect of recycling noted in literature is a weakened mechanical response. Therefore, a discussion with other literature examples is needed to put our work into perspective and attempt to explain these contrasting observed behaviors.

In the work of Spinacé et al. [17] and La Mantia et al. [15], a complete loss of ductility was observed after, respectively, three and one recycling cycles in a single-screw extruder. In both researches, a crystallinity increase was noticed. Mancini et al. [63] also showed a total loss of ε_{break} as crystallinity increase from 23 to 37% after five injection molding and grinding cycles. In this article, the chain scission of PET was probably more severe than in our study, since the acid content increase from 40 (vPET) to 130 mmol/kg (rPET-C5). Moreover, we could argue that these differences could originate from the different processing used for recycling.

Interestingly, other articles with a more alike protocol to ours (co-rotating twin screw extruder), observed a loss of plastic properties as well [13, 19]. In the work of Badia et al. [13], however, the main reason is a very sharp crystallinity increase of around 34% after three cycles, much more substantial than in our case (around 7.5%). No information was given about the extent of degradation. Wu et al. [19] showed a more modest crystallinity increase of 17% after three cycles, with a similar Mw loss to our study (from vPET = 60 kg/mol to rPET-C3 = 33 kg/mol). However, the used samples for testing were not as amorphous as in our case (initial χ_c are usually at levels of 22% up to 43%) and the tensile test speed are higher (10 mm/min for Wu et al [19] for example). Indeed, presumably the slow tensile testing speed (5 mm/min in our case) allows a sufficient time for the chains to accommodate the applied load and give a ductile response [64, 65]. In the cited examples, the effect of physical aging on the final mechanical response is never addressed although an embrittlement is expected with increasing densification of polymer chains [25, 26, 66].

As can be seen, comparing the obtained results with literature is always a challenge since the processing used for the production of rPET (instrument and used conditions, drying protocol, etc.), the initial crystallinity and the mechanical testing conditions (speed and physical aging) are considerably different. Added to that, when a similar processing is used, morphological changes are rarely put into perspective with mechanical characterization for rPET. Finally, the unclear definition of Mc makes it even harder to establish the transition to a fragile regime. There- fore, the hypothesis of a competition between crystallinity increase and chain cleavages (still allowing a sufficient entanglement for plastic deformation) appears well-founded and do not contradict other literature examples.

Impact resistance

The notched impact resistance was studied for injected vPET and rPET-C5. The results in Table 10 depict a characteristic behavior of a very fragile material. The resilience stayed almost constant at 3.7 KJ/m^2, with an increase in the standard deviation for five-time reprocessed samples. This can probably be linked to the difficulty in injection molding of these samples and the presence of defects (air bubbles or shrinking). Plus, because of the thickness of these specimens, the homogeneity of their cooling in the mold was more difficult and it was slow in their core. A whitening of the internal part of the impact bars was observed for rPET-C5 compared to vPET (see Figure S4 in Supporting Information), probably indicating the presence of shear-induced crystallization.

Anyhow, these results are in accordance with the literature [50, 63], as PET (and semi-crystalline polyesters in general) is known as a notch-sensitive material, with a fracture mechanism driven by a craze propagation [67]. The injection molding conditions could be optimized in another instrument, but are not expected to change remarkably since non-formulated PET tend to have a low impact resistance.

Table 10: Mechanical testing data, impact strength of notched samples after injection without aging.

Sample	Impact Strenght (kJ/m2)
vPET	3.8 ± 0.6
rPET-C5	3.6 ± 1.5

4 Conclusion

In this work, the mechanical recycling of PET was simulated via successive extrusion cycles up to five times. During processing, degradation mechanisms triggered by shearing at high temperatures, oxygen or humidity, resulted in several structural modifications and unstable processing. A strong chain scission induced a constant viscosity decrease along with a slight branching. The presence of formed chromophoric structures was also used to quantify the state of degradation, since a visible yellowing and a significant color changes increased with recycling.

The microstructure modification caused by recycling had a noticeable effect on the crystallization kinetics, especially after injection molding. The presence of shorter mobile chains and impurities from processing, favored their packing and therefore the overall organization in a crystal phase. An increase in both crystallization temperature and crystallinity was noticed by DSC, with the formation of two crystal populations and higher nucleation speeds. Surprisingly, even if rPET has modified properties, the mechanical response stayed similar to the virgin material.

On uniaxial tensile tests, rPET kept an overall ductility (ε_{break} > 400%) even with a slight increase of the Young's modulus. The impact strength, as expected, remained at 3.7 kJ/m^2 range, witnessing the well-described notch-sensitivity of polyester materials. These results allowed to point out that the molecular weight changes alone did not govern the mechanical behavior. Presumably, this phenomenon can be linked to a remaining entanglement since the critical molar mass was not reached during five recycling cycles, allowing a ductile response.

This work allowed to bring to light that the main issue of mechanically recycled PET is not the loss of mechanical properties, as often simplified in literature, but the challenges in fabricating the recyclates. In the laboratory conditions, the growing difficulty of processing and instability was the greater barrier for the increasing number of cycles, whereas the tensile or impact resistance were practically constant all along. To complete this study, it would be interesting to use bottle scraps from the industry instead of a vPET to provide insights on the effect of a life-cycle before recycling. Plus, comparing results with industrially recycled processes would allow establishing potential parallels in terms of final properties.

Supporting information

This information is available free of charge via the Internet at https://pubs.acs.org/...
Residual humidity of vPET, SEC results, TGA measurements and results, Picture of a specimen of rPET-C5.

Acknowledgements

The authors gratefully acknowledge the "Association Nationale de la Recherche et de la Technologie" (France) for funding the PhD thesis of Gabriela Gonçalves Marques (CIFRE # 2021/1131).

References

[1] Geyer, R.; Jambeck, J.R.; Law, K. L. Production, use, and fate of all plastics ever made. *Sci Adv.* **2017**, *3*, e1700782.

[2] Damayanti; Wu, H.-S. Strategic possibility routes of recycled PET. *Polymers* **2021,** *13*, 1475.

[3] Welle, F. Twenty years of pet bottle to bottle recycling—an overview. *Resour. Conserv. Recycl.* **2011**, *55*, 865–875

[4] Tiwari, R.; Azad, N.; Dutta, D.; Yadav, B. R.; Kumar, S. A critical review and future perspective of plastic waste recycling. *Sci. Total Environ.* **2023**, *881*, 163433.

[5] Schyns, Z. O. G.; Shaver, M. P. Mechanical recycling of packaging plastics: A review. *Macromol. Rapid Commun*. **2021**, *42*, 2000415

[6] Hundertmark, T.; Mayer, M.; McNally, C.; Simons, T. J.; Witte, C. How plastics waste recycling could transform the chemical industry. *McKinsey & Company* **2018**, *12*, 1–11

[7] Hopewell, J.; Dvorak, R.; Kosior, E. Plastics recycling: challenges and opportunities. *Philos. Trans. R. Soc. B* **2009**, *364*, 2115–2126

[8] Sarda, P.; Hanan, J. C.; Lawrence, J. G.; Allahkarami, M. Sustainability performance of polyethylene terephthalate, clarifying challenges and opportunities. *J. Polym. Sci.* **2022**, *60*, :7–31

[9] Awaja, F., Pavel, D. Recycling of PET. *Eur. Polym. J.* **2005**, *41,* 1453–1477

[10] Long, T. E.; Scheirs, J. *Modern polyesters: chemistry and technology of polyesters and copolyesters*. John Wiley & Sons Ltd: Chichester, England, 2003.

[11] Negoro, T.; Thodsaratpreeyakul, W.; Takada, Y.; Thumsorn, S.; Inoya, H.; Hamada, H. Role of crystallinity on moisture absorption and mechanical performance of recycled PET compounds. *Energy Procedia* **2016**, *89*, 323–327

[12] Assadi, R.; Colin, X.; Verdu, J. Irreversible structural changes during pet recycling by extrusion. *Polymer* **2004**, *45*, 4403–4412

[13] Badia, J.D.; Vilaplana, F.; Karlsson, S.; Ribes-Greus, A. Thermal analysis as a quality tool for assessing the influence of thermo-mechanical degradation on recycled poly (ethylene terephthalate). *Polym. Test.* **2009**, *28*, 169–175

[14] Frounchi, M. Studies on degradation of pet in mechanical recycling. *Macromol. Symp.* **1999**, *144*, 465–469

[15] La Mantia, F. P.; Vinci, M. Recycling poly (ethyleneterephthalate). *Polym. Degrad. Stab.* **1994**, *45*, 121–125

[16] Nait-Ali, L. K.; Colin, X.; Bergeret, A. Kinetic analysis and modelling of pet macromolecular changes during its mechanical recycling by extrusion. *Polym. Degrad. Stab.* **2011**, *96*, 236–246

[17] Silva Spinacé, M.A. ; De Paoli, M.A. Characterization of poly (ethylene terephtalate) after multiple processing cycles. *J. Appl. Polym. Sci.* **2001**, *80*, 20–25

[18] Wang, W.; Taniguchi, A.; Fukuhara, M.; Okada, M. Surface nature of uv deterioration in properties of solid poly (ethylene terephthalate). *J. Appl. Polym. Sci.* **1998**, *67*, 705–714

[19] Wu, H.; Lv, S.; He, Y.; Qu, J. P. The study of the thermomechanical degradation and mechanical properties of

pet recycled by industrial-scale elongational processing. *Polym. Test.* **2019**, *77*, 105882

[20] Del Mar Castro López,Pernas, M.; A.I.A.; López, M. J. A.; Lasagabaster Latorre, A.; López Vilariño, J.M.. González Rodríguez, M.V. Assessing changes on poly (ethylene terephthalate) properties after recycling: Mechanical recycling in laboratory versus postconsumer recycled material. *Mater. Chem. Phys.* **2014**, *147*, 884–894

[21] Berg, D.; Schaefer, K.; Moeller, M. Impact of the chain extension of poly (ethylene terephthalate) with 1, 3-phenylene-bis-oxazoline and n, n-carbonylbiscaprolactam by reactive extrusion on its properties. *Polym. Eng. Sci.* **2019**, *59*, 284–294

[22] Inata, H. ; Matsumura, S.Chain extenders for polyesters. v. reactivities of hydroxyl-addition-type chain extender; 2, 2-bis (4h-3, 1-benzoxazin-4-one). *J. Appl. Polym. Sci.* **1987**, *34*, 2609–2617

[23] Villalobos, M.; Awojulu, A.; Greeley, T.; Turco, G.; Deeter, G. Oligomeric chain extenders for economic reprocessing and recycling of condensation plastics. *Energy* **2006**, *31*, 3227–3234

[24] Celik, Y.; Shamsuyeva, M.; Endres, H.J.Thermal and mechanical properties of the recycled and virgin pet—part i. *Polymers* **2022**, *14*, 1326

[25] Browstow, R.W.; Corneliussen, W; *Failure in Plastics*. Hanser Publishers, 1986.

[26] Struik, L.C.E.; Mechanical behaviour and physical ageing of semi-crystalline polymers: 4. *Polymer* **1989**, *30*, 815–830.

[27] Zhou, H.; Lofgren, E. A.; Jabarin, S.A. Effects of microcrystallinity and morphology on physical aging and its associated effects on tensile mechanical and environmental stress cracking properties of poly(ethylene terephthalate). *J. Appl. Polym. Sci.* **2009**, *112*, 2906–2917.

[28] Zimm, B.E; Stockmayer, W.H.; Fixman, F. Excluded volume in polymer chains. *J. Chem. Phys.*, **1953**, *21*, 1716–1723

[29] Li, Y.; Yao, Z.; Qiu, S.; Zeng, C.; Cao, K. Influence of molecular structure on the rheological properties and foamability of long chain branched polypropylene by "one-pot" reactive extrusion. *J Cell. Sci.* **2021**, *57*, 433–449

[30] Solomon, O.F.; Ciută, I.Z. Détermination de la viscosité intrinsèque de solutions de polymères par une simple détermination de la viscosité. *J. Appl. Polym. Sci.* **1962**, *6*, 683–686.

[31] Pinter, E.; Welle, F.; Mayrhofer, E.; Pechhacker, A.; Motloch, L.; Lahme, V.; Grant, A.; Tacker, M. Circularity study on pet bottle-to-bottle recycling. *Sustainability* **2021**, *13*, 7370.

[32] Mehta, A.; Gaur, U. ; Wunderlich, B. Equilibrium melting parameters of poly (ethylene terephthalate). *J. Polym. Sci., Polym. Phys. Ed.* **1978**, *16*, 289–296

[33] Cardi, N.; Po, R.; Giannotta, G. ; Occhiello, E.; Garbassi, F.; Messina, G. Chain extension of recycled poly (ethylene terephthalate) with 2, 2-bis (2-oxazoline). *J. Appl. Polym. Sci.* **1993,** *50*, 1501–1509

[34] Colin, X.; Tcharkhtchi, A. Thermal degradation of polymers during their mechanical recycling. In *Recycling: Technological Systems, Management Practices and Environmental Impact,* Ed. Culleri J. C. Nova Science, 2013, pp 57–95

[35] Paci, M.; La Mantia, F.P. Competition between degradation and chain extension during processing of reclaimed poly (ethylene terephthalate). *Polym. Degrad. Stab.* **1998**, *61*, 417–420

[36] Launay, A.; Thominette, F.; Verdu, J. Hydrolysis of poly (ethylene terephthalate). a steric exclusion chromatography study. *Polym. Degrad. Stab.* **1999**, *63*, 385–389

[37] Zimmerman, H.; Kim, N.T. Investigations on thermal and hydrolytic degradation of poly (ethylene terephthalate). *Polym. Eng. Sci.* **1980**, *20*, 680–683

[38] Rothen-Weinhold, A.; Besseghir, K.; Vuaridel, E.; Sublet, E. ; Oudry, N.; Kubel, F.; Gurny, R.. Injection-molding versus extrusion as manufacturing technique for the preparation of biodegradable implants. *Eur J Pharm Biopharm.* **1999**, *48*, 113–121

[39] Takahashi, H.; Matsuoka, T.; Kurauchi, T. Rheology of polymer melts in high shear rate. *J. Appl. Polym. Sci.* **1985**, *30*, 4669–4684

[40] Rieckmann, T.; Besse, K.; Frei, F.; Völker, S. Quantification of colour formation in PET depending on ssp residence time, temperature, and oxygen concentration. *Macromol. Symp.* **2013**, *333*, 162–171

[41] Ciolacu, C. F. L.; Choudhury, N. R. Dutta, N. K. Colour formation in poly (ethylene terephthalate) during melt processing. *Polym. Degrad. Stab.* **2006**, *91*, 875–885

[42] Berg, D.; Schaefer, K.; Koerner, A.; Kaufmann, R.; Tillmann, W.; Moeller, M. Reasons for the discoloration of postconsumer poly (ethylene terephthalate) during reprocessing. *Macromol. Mater. Eng*. **2016**, *301*, 1454–1467, 2016.

[43] Zimmermann, H.; Leibnitz, E. Chemische untersuchungen über faserbildende polyester. *Faserforsch Textil- tech.* **1965,** *16*, 282–290.

[44] Edge, M.; Allen, N.S.; Wiles, R.; McDonald, W.; Mortlock, S.V. Identification of luminescent species contributing to the yellowing of poly (ethyleneterephthalate) on degradation. *Polymer*, **1995**, *36*, 227–234

[45] Edge, M.; Wiles, R.; Allen, N.S.; McDonald, W.; Mortlock. S.V. Characterisation of the species responsible for yellowing in melt degraded aromatic polyesters—i: Yellowing of poly (ethylene terephthalate). *Polym. Degrad. Stab*. **1996**, *53*(2), 141–151

[46] Gupta, V.B.; Bashir, Z. in *Handbook of Thermoplastic Polyesters: Homopolymers, Copolymers, Blends, and Composites,* Ed. Fakirov S. 2002, Chap.7, pp 317-388 : *PET fibers, films, and bottles.*

[47] Alongi, J.; Ciobanu, M.; Tata, J.; Carosio, F. ; Malucelli, C. Thermal stability and flame retardancy of polyester, cotton, and relative blend textile fabrics subjected to sol–gel treatments. *J. Appl. Polym. Sci.* **2011**, *119*, 1961–1969

[48] Candal, M.V.; Safari, M.; Fernández, M.; Otaegi, I.; Múgica, A.; Zubitur, M.; Gerrica-Echevarria, G.; Sebastián, V.; Irusta, S.; Loaeza, D. Structure and properties of reactively extruded opaque post-consumer recycled PET *Polymers* **2021**, *13*, 3531

[49] Badia, J.D.; Strömberg, E; Karlsson, S.; Ribes-Greus, A. The role of crystalline, mobile amorphous and rigid amorphous fractions in the performance of recycled poly (ethylene terephthalate) (PET). *Polym. Degrad. Stab*. **2012**, *97*, 98–107

[50] Torres, N.; Robin, J.J.; Boutevin, B. Study of thermal and mechanical properties of virgin and recycled poly (ethylene terephthalate) before and after injection molding. *Eur. Polym. J.* **2000**, *36*, 2075–2080.

[51] Katarzyna Polak-Kraśna, Ali Reza Abaei, Reyhaneh Neghabat Shirazi, Eoin Parle, Oliver Carroll, William Ronan, and Ted J Vaughan. Physical and mechanical degradation behaviour of semi-crystalline plla for bioresorbable stent applications. *J. Mech. Behav. Biomed. Mater.* **2021,** *118*, 104409.

[52] Mancini, S. D.; Zanin, M. Consecutive steps of pet recycling by injection: evaluation of the procedure and of the mechanical properties. *J. Appl. Polym. Sci.* **2000**, *76*, 266–275

[53] Jabarin, S.A. Crystallization kinetics of polyethylene terephthalate. i. isothermal crystallization from the melt. *J. Appl. Polym. Sci.* **1987**, *34*, 85–96

[54] Blair Crawford, C. ; Quinn, B. *Microplastic pollutants*. Elsevier Limited, 2017.

[55] Wunderlich, B. *Macromolecular Physics, Vol 1: Crystal Structure, Morphology, Defects - Chap 3*, Academic Press: New York and London, 1973.

[56] Perkins, W.G. Polymer toughness and impact resistance. *Polym. Eng. Sci*. **1999**, *39*, 2445– 2460

[57] Ohlberg, S.M.; Roth,J.; Raff, R.A.V. Relationship between impact strength and spherulite growth in linear polyethylene. *J. Appl. Polym. Sci.* **1959**, *1*, 114–120

[58] Farrar, D.F; Gillson, R.K. Hydrolytic degradation of polyglyconate b: the relationship between degradation time, strength and molecular weight. *Biomaterials* **2002**, *23*, 3905–3912

[59] Dzieciol, M.; Trzeszczynski, J. Studies of temperature influence on volatile thermal degradation products of poly (ethylene terephthalate). *J. Appl. Polym. Sci*. **1998**, *69*, 2377–2381

[60] Liu, Y.; Xu, H.; Liu, G.; Pu, S.. Core/shell morphologies in recycled poly (ethylene terephthalate)/linear low-density polyethylene/poly (styrene-b-(ethylene-co-butylene)-b-styrene) ternary blends. *Polymer Bulletin* **2017**, *74*, 4223–4233.

[61] Bocz, K.; Ronkay, F.; Decsov, K. E.; Molnár, B.; Marosi, G. Application of low-grade recyclate to enhance reactive toughening of poly (ethylene terephthalate). *Polym. Degrad. Stab.* **2021**, *185*, 109505

[62] Zong, Y.; Cheng, Y.; Dai, G. The relationship between rheological behavior and toughening mechanism of toughened poly (ethylene terephthalate*). J. Compos. Mater.* **2008**, *42*, 1571–1585

[63] Mancini, S. D.; Zanin, M. Recyclability of PET from virgin resin. *Mater. Res.* **1999**, *2*, 33–38.

[64] Kausch, H. H.; DeVries, K. L. Molecular aspects of high polymer fracture as investigated by esr-technique. *Int. J. Fract.*, **1975**, *11*, 727–759.

[65] Kausch, H. H. *Polymer fracture*, vol. 2, Springer Science & Business Media, **2012**.

[66] Zhou, H.; Lofgren, E. A.; Jabarin, S.A. Effects of microcrystallinity and morphology on physical aging of poly (ethylene terephthalate). *J. Appl. Polym. Sci.* **2007**, *106*, 3435–3443.

[67] Loyens, W.; Groeninckx, G. Ultimate mechanical properties of rubber toughened semicrystalline pet at room temperature. *Polymer* **2002**, *43*, 5679–5691